PROCEEDINGS of the
23rd International Congress on Acoustics
9 to 13 September 2019 in Aachen, Germany

Robust stability and performance of local active control systems using virtual sensing

Stephen ELLIOTT[1]*, Chung Kwan LAI[1], Thibault VERGEZ[2], Jordan CHEER[1]

[1]ISVR, University of Southampton, United Kingdom

[2]École Centrale de Lyon, France

ABSTRACT

Local active noise control systems often use virtual sensing techniques; to estimate the pressure to be controlled at the listener's ears from an array of remote monitoring microphones for example. The virtual sensing process inevitably makes assumptions about the acoustic environment, although the environment is generally subject to uncertainties under different operating conditions. This paper considers the performance and stability of the remote microphone technique, as an example of a virtual sensing method, in a vehicle when subject to uncertainties due to changes in the internal acoustics and road conditions. It is shown, using data from experiments in a vehicle, that both the robust stability and the robust performance are improved by using regularisation in the design of the filter used to estimate the pressure at the listener's ears from the outputs of the array of monitoring microphones.

Keywords: active control, local sound control, virtual sensing

1 INTRODUCTION

Although local systems for the active attenuation of sound at the listener's ear date back to the 1950s (1), they have recently attracted renewed interests due to the possibility of using head tracking methods and virtual sensing to extend their frequency range (2, 3, 4). When applied to local active sound control, the virtual sensing problem involves estimating the sound pressure at the listener's ear using the signals from an array of static monitoring microphones, via an "observation" filter, as shown in Figure 1. For applications such as the control of road noise in vehicles, the signals are random and spectral density methods can be used to predict the active control performance (5), particularly if the control system is designed to minimise the delayed error, so that some of the causality problems can be avoided (6, 7). The adaptive feedforward control algorithm typically used in these applications, as shown in Figure 2 (6, 8), not only uses an internal model of the responses from the secondary loudspeakers to the microphones, but also makes assumptions about the primary sound field under control in the design of the observation filters (9). As the upper frequency of control is extended using head tracking, the uncertainties associated with these responses tends to increase, threatening the stability and performance of the control system. In this paper, the responses measured in a car under different environmental conditions are used to investigate how the stability and performance can be made robust to such uncertainties, in particular using regularisation in the design of the observation filter.

2 ADAPTIVE FEEDFORWARD CONTROL USING VIRTUAL SENSING

In this paper it is assumed that the remote microphone technique is used for virtual sensing, together with an adaptive feedforward control system, to give the block diagram shown in Figure 2. The observation filter, $\boldsymbol{O}$, is assumed to be designed in the frequency domain to minimise the expected mean square difference between the estimated disturbance signal at the virtual microphone, $\hat{\boldsymbol{d}}_e$, and the true

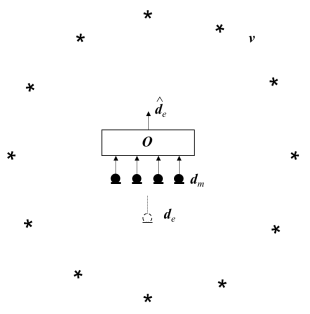

Figure 1 – The primary disturbance signal, $\boldsymbol{d}_e$, at a virtual microphone, which is due to an array of primary sources, $\boldsymbol{v}$,is estimated using the signals from an array of monitoring microphones, $\boldsymbol{d}_m$, via an observation filter, $\boldsymbol{O}$, to give the estimate $\hat{\boldsymbol{d}}_e$.

*sje@isvr.soton.ac.uk

disturbance signal, $\boldsymbol{d}_e$, so that the optimum matrix of filters is given by (5, 9)

$$\boldsymbol{O}_{opt} = \boldsymbol{S}_{d_m d_e}(\boldsymbol{S}_{d_m d_m} + \beta \boldsymbol{I})^{-1} \tag{1}$$

where $\boldsymbol{S}_{d_m d_e}$ and $\boldsymbol{S}_{d_m d_m}$ are spectral density matrices defined as $\boldsymbol{S}_{d_m d_e} = E[\boldsymbol{d}_e \boldsymbol{d}_m^H]$ and $\boldsymbol{S}_{d_m d_m} = E[\boldsymbol{d}_m \boldsymbol{d}_m^H]$, $E[\ ]$ is the expectation operator and β is a regularisation parameter. The adaptive feedforward control system shown in Figure 2 can be shown to be stable, for slow adaptation, if the following condition is satisfied (4),

$$\text{Re}\left(\text{eig}\left[\hat{\boldsymbol{G}}_e^H \hat{\boldsymbol{G}}_e + \hat{\boldsymbol{G}}_e^H \hat{\boldsymbol{O}}_{opt}\left(\boldsymbol{G}_m - \hat{\boldsymbol{G}}_m\right)\right]\right) > 0 \tag{2}$$

when $\boldsymbol{G}_e$ and $\hat{\boldsymbol{G}}_e$ are the true and estimated values of the responses between the secondary sources and the error microphones, $\boldsymbol{G}_m$ and $\hat{\boldsymbol{G}}_m$ are the true and estimated values of the responses between the secondary sources and the monitoring microphones and $\boldsymbol{O}_{opt}$ is given by Eq.(1). If the adaptive controller is sable, and converges to minimise the expectation of the mean square value of the estimated error, $E[\hat{\boldsymbol{e}}^H \hat{\boldsymbol{e}}]$, it can be shown that the spectral density matrix of the true error at the virtual microphones, $E[\boldsymbol{e}^H \boldsymbol{e}]$, is given by

$$\begin{aligned}\boldsymbol{S}_{ee} =& \boldsymbol{S}_{d_e d_e} - \boldsymbol{G}_e(\boldsymbol{G}^H\boldsymbol{G})^{-1}\boldsymbol{G}^H\hat{\boldsymbol{O}}_{opt}\boldsymbol{S}_{d_m d_e}^H - \boldsymbol{S}_{d_m d_e}\hat{\boldsymbol{O}}_{opt}^H\boldsymbol{G}(\boldsymbol{G}^H\boldsymbol{G})^{-1}\boldsymbol{G}_e^H \\ &+\boldsymbol{G}_e(\boldsymbol{G}^H\boldsymbol{G})^{-1}\boldsymbol{G}^H\hat{\boldsymbol{O}}_{opt}\boldsymbol{S}_{d_m d_m}\hat{\boldsymbol{O}}_{opt}^H\boldsymbol{G}(\boldsymbol{G}^H\boldsymbol{G})^{-1}\boldsymbol{G}_e^H .\end{aligned} \tag{3}$$

where $\boldsymbol{G} = \hat{\boldsymbol{G}}_e + \hat{\boldsymbol{O}}_{opt}(\boldsymbol{G}_m - \hat{\boldsymbol{G}}_m)$ and so the optimal attenuation at all the virtual error senses is given by

$$L_e = -10\log_{10}\left|\frac{trace\{\boldsymbol{S}_{ee}\}}{trace\{\boldsymbol{S}_{d_e d_e}\}}\right| . \tag{4}$$

The choice of the regularisation parameter in Eq.(1) is thus a trade-off between good performance, i.e. a low value of L_e, and robust stability, i.e. ensuring that the norm of $\boldsymbol{O}_{opt}$ is not so large that small values of $(\boldsymbol{G}_m - \hat{\boldsymbol{G}}_m)$ cause the real parts of any of the eigenvalues in Eq.(2) to become negative.

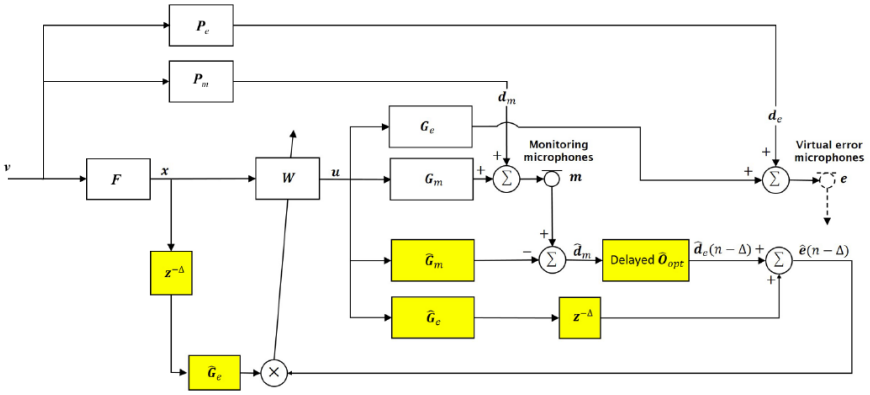

Figure 2 – Block diagram of an adaptive feedforward control system using the remote microphone method with a modelling delay, in yellow, as a virtual sensing method to estimate the error signal at the virtual microphones, $\boldsymbol{e}$, from the signals at the monitoring microphones, $\boldsymbol{m}$.

3 PREDICTING ROBUST STABILITY AND PERFORMANCE FROM MEASUREMENTS IN A VEHICLE

A series of measurements was taken in a medium-sized car (Hyundai i40) with two secondary loudspeakers attached to the headrest on the left-hand front seat, as shown in Figure 3a, and five loudspeakers at different positions on the floor, which were assumed to act as primary sources when each was driven with uncorrelated white noise. Four microphones on the headrest were used as the monitoring sensors and two microphones in the ears of a Neumann KU100 dummy head, positioned close to the headrest, were used as the true error signals, as shown in Figure 3b. The frequency responses from all of the loudspeakers to all of the microphones were measured under a number of different conditions in the vehicle,

in particular when the left-hand front seat, seat 1, was in its mid position (Nominal) and when moved as far as possible from the steering wheel (Perturbed). In order to more clearly see the effect of such a perturbation on the stability and performance, the changes in the responses due to the seat movements were enhanced by multiplying the differences between the two measured responses by a factor of two. Figure 4 shows the frequency responses from one of the secondary sources to one of the monitoring microphones under these two conditions. It can be seen that this perturbation changes both the magnitude and the phase of the frequency response, particularly at high frequencies. If the observation filter is designed for the nominal condition, with the regularisation factor of β, but is then used in the perturbed vehicle condition, both the performance and stability of the control system will be affected to different extents, depending on the value of β.

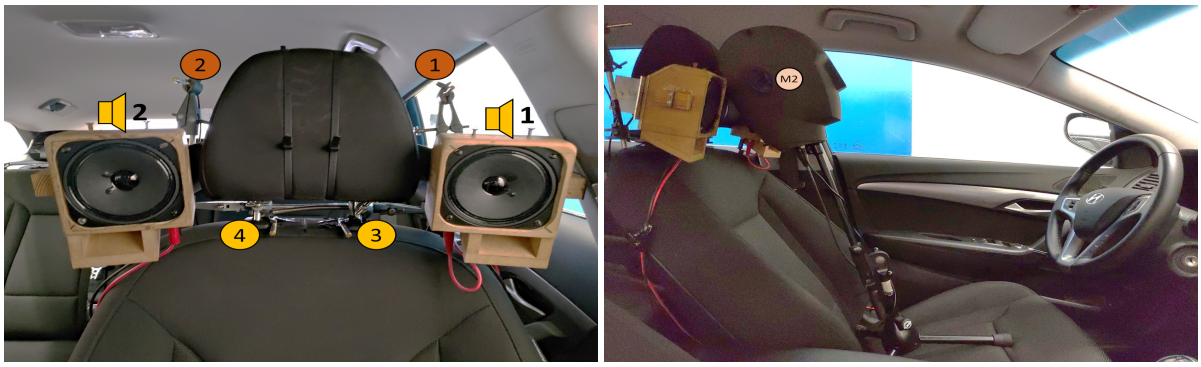

(a) (b)

Figure 3 – The arrangement of loudspeakers used as secondary sources and monitoring microphones on the headrest of the front left seat of the test vehicle (a) and the position of the dummy head in which the virtual error microphones were mounted (b).

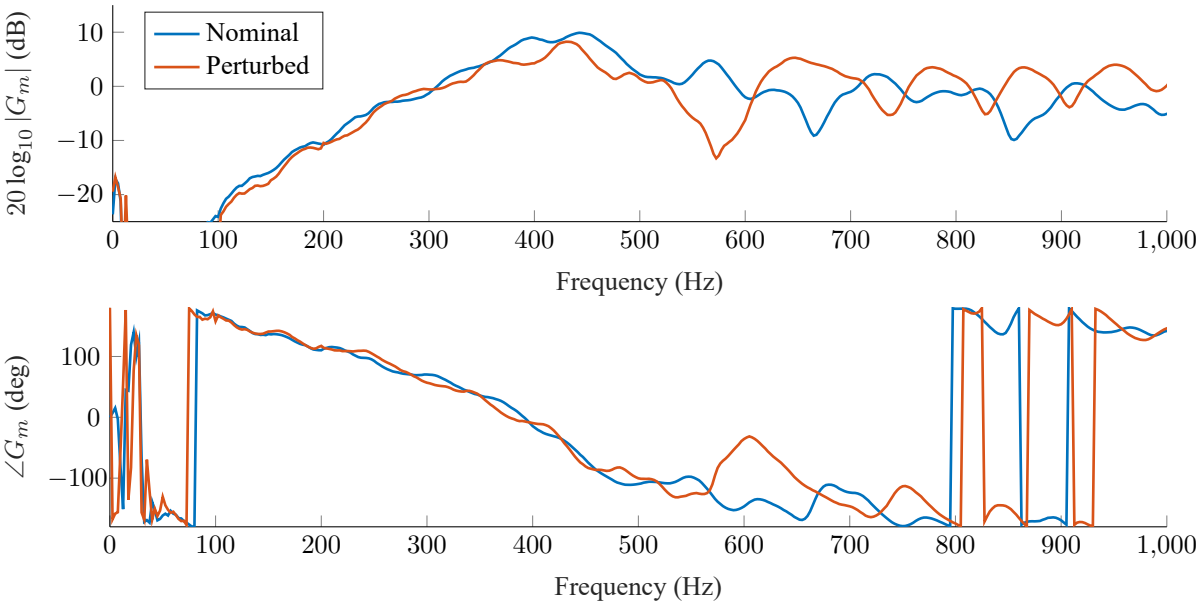

Figure 4 – Magnitude and phase in degrees of the frequency response from one of the secondary sources to one of the monitoring microphones when seat 1 was in its mid position, Nominal, and when in an altered position, Perturbed.

Figure 5 shows the real parts of the two eigenvalues of Eq.(2) as a function of frequency, calculated using the nominal and perturbed frequency responses measured in the vehicle and when the observation filter in Eq.(1) is calculated from the nominal frequency responses, but with two values of the regularisation parameter, β. It can be seen that if β is very small, 10^{-5}, as in Figure 5a, one of the eigenvalues becomes negative at a number of frequencies, including 960 Hz, indicating that the adaptive control system would be unstable. When the regularisation factor is increased to 10^{-3}, as in Figure 5b, however, both eigenvalues are positive at all frequencies, and so that the system would then be stable.

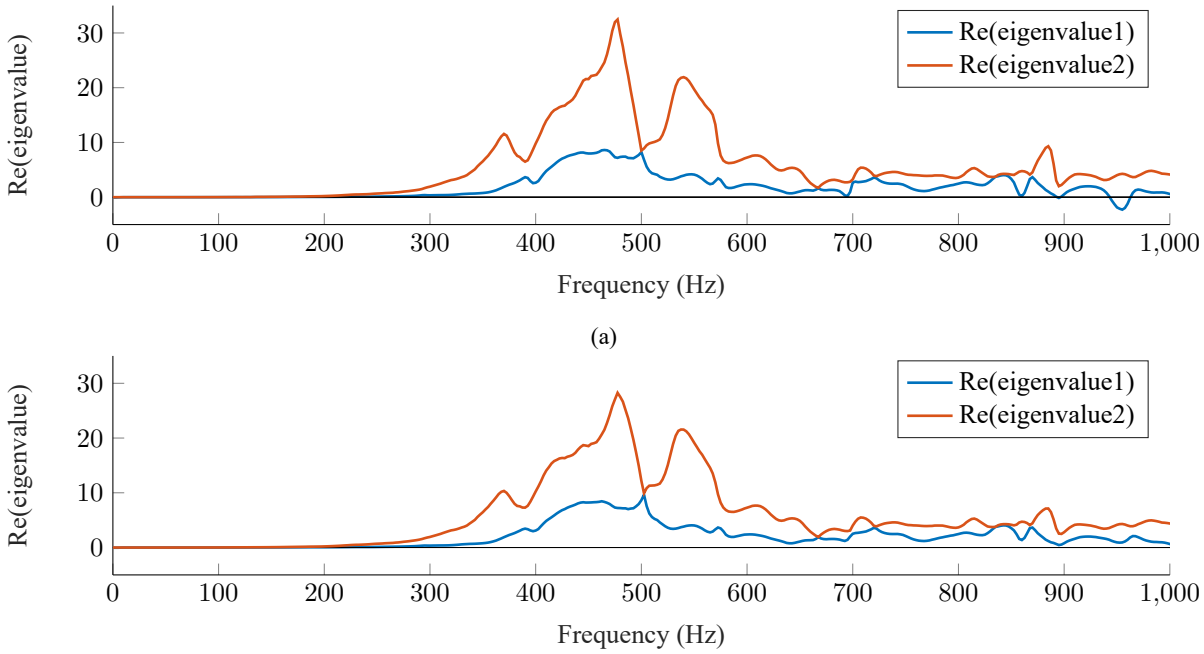

(a)

(b)

Figure 5 – The real parts of the two eigenvalues of Eq.(2) evaluated from the measurements made in the vehicle under nominal and perturbed conditions, when the observation filter was designed with two values of the regularisation parameter, β.

Figure 6a shows the variation of the real parts of the two eigenvalues with the observation filter regularisation parameter β, at the single frequency of 960 Hz. It can be seen that both eigenvalues are positive for values of β greater than about 3×10^{-4}. Figure 6b shows the variation with beta of the predicted attenuation performance at the two error microphones, in Eq.(4). This graph is not really useful for values of β below 3×10^{-4}, since the system is then unstable and a frequency domain calculation of the error is not valid, but above this value, when the system is stable, the attenuation is about 4 dB for values of β of about 10^{-3} and then falls off at higher values. It is clear that not only can the control system be made more robustly stable if the observation filter is designed with an appropriate value of the regularisation parameter, but this can also ensure robust performance.

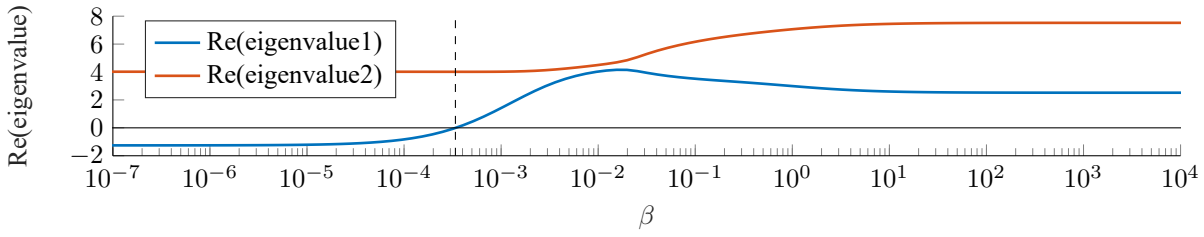

(a)

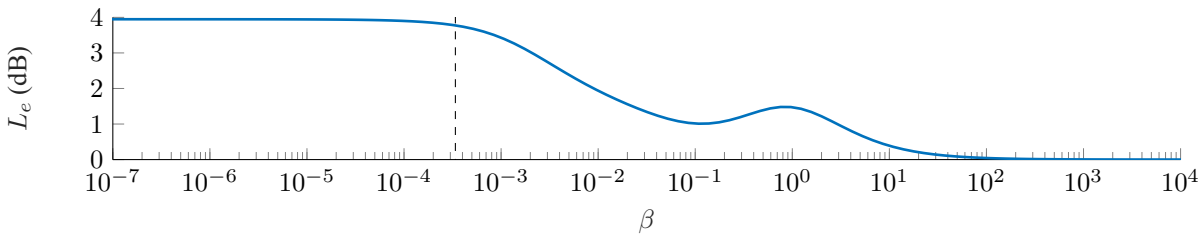

(b)

Figure 6 – The variation of the real parts of the two eigenvalues in Eq.(2), evaluated at a frequency of 960 Hz, (a) and the attenuation in the sum of squared error signals at this frequency (b), as a function of the regularisation parameter, β.

4 CALCULATION OF THE EFFECT OF MULTIPLE SIMULTANEOUS UNCERTAINTIES FROM MEASUREMENTS OF INDIVIDUAL UNCERTAINTIES

The practical design of a control system using virtual sensing should involve testing its robust stability and performance under all the perturbed conditions, which give rise to uncertainties in the responses, that are likely to be encountered in practice. If, for example, there are 10 potential sources of uncertainty then the number of potential conditions under which the response needs to be measured will be the nominal one, 10 conditions in which only one uncertainty is acting alone, 45 conditions in which there are two different combinations of uncertainties, and so on. The total number of conditions for different numbers of the 10 sources uncertainty acting together is thus about 1,000. The number of potential measurements that need to be made could thus become very large and it is of interest to examine whether the effects of some of these simultaneous perturbations, due to multiple sources of uncertainty, could be estimated from the individual uncertainties, measured on their own.

Figure 7 shows the measured frequency response from a secondary source to a monitoring microphone under four different conditions: nominal, with the response perturbed by lowering seat 2, the front-right seat, only, with the response perturbed by lowering seat 3, the rear-left seat, only, and with the results perturbed by lowering both seats 2 and 3.

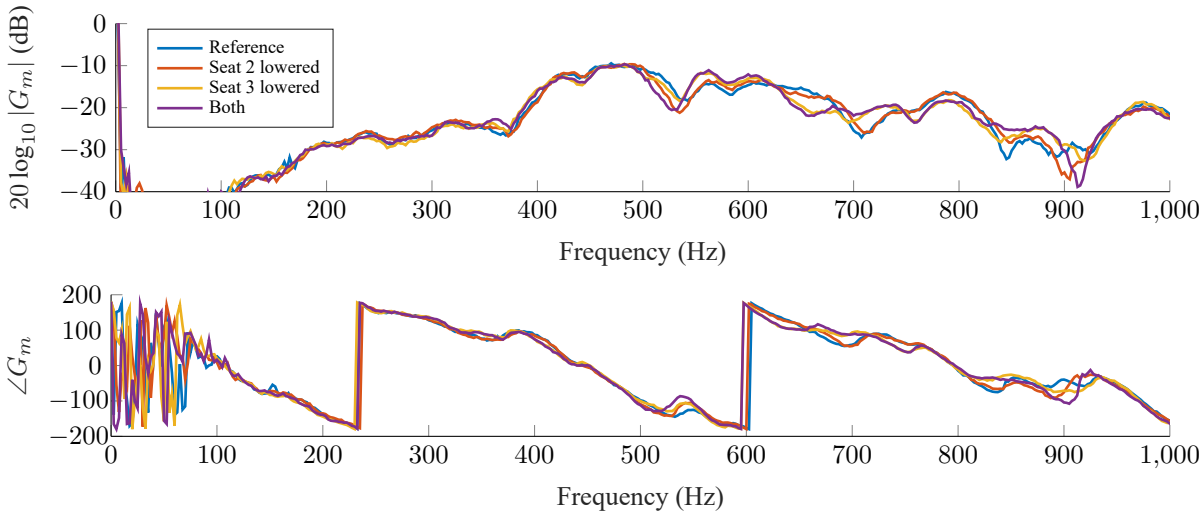

Figure 7 – Responses measured from a secondary loudspeaker to a monitoring microphone under nominal conditions, Reference, when seat 2 only is lowered, when seat 3 only is lowered and when both seats 2 and 3 are both lowered.

The question is whether the effect of both perturbations acting together can be predicted from the two perturbations acting alone. Let G_0 be the response under nominal conditions and write the responses with the effects of the first and second perturbations acting individually as

$$G_1 = G_0 + \Delta G_1 \quad , \quad G_2 = G_0 + \Delta G_2 \tag{5}$$

where ΔG_1 and ΔG_2 are the additive uncertainties. Also write the response when these two perturbations act together as

$$G_{1,2} = G_0 + \Delta G_{1,2}. \tag{6}$$

The question is whether $\Delta G_{1,2}$ can be estimated from ΔG_1 and ΔG_2, and hence whether $G_{1,2}$ can be estimated from G_0, G_1 and G_2. One way of estimating $G_{1,2}$ would be just to use the superposition of ΔG_1 and ΔG_2, so that

$$\hat{\Delta} G_{1,2} = \Delta G_1 + \Delta G_2. \tag{7}$$

Figure 8 shows a comparison of $\Delta G_{1,2}$ and $\hat{\Delta} G_{1,2}$ calculated from the measured data in Figure 7. It can be seen that a reasonably good approximation to the effect of the two perturbations acting together can be obtained from the superposition of the individual perturbations. Although, from a frequency domain perspective, there does not appear to be any obvious reason for the superposition of the individual uncertainties, there does seem to be some justification in the time domain, in terms of the individual impulse responses. Consider the case in which the uncertainties are generated by two reflecting objects.

In the time domain ΔG_1 and ΔG_2 correspond to the additional reflections measured at the microphone, generated by reflections from the source due to either object 1 or object 2 individually. If both objects are present, the impulse response will contain additional reflections due to object 1 and additional reflections due to object 2, and so superposition of the uncertainties would hold except for the later reflections of both object 1 and object 2, which will generally be small compared to the earlier reflections.

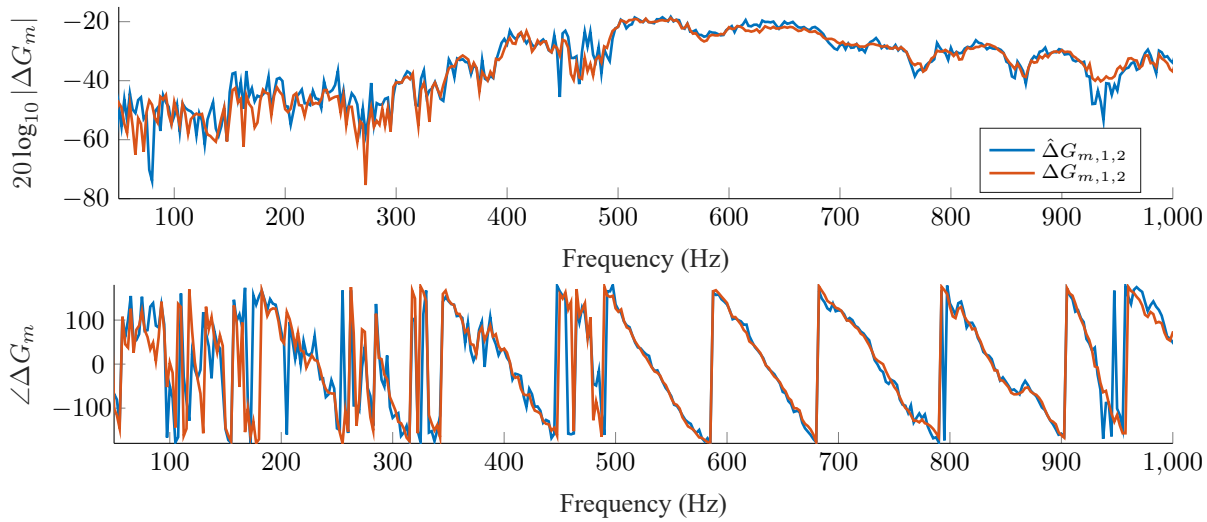

Figure 8 – The additive uncertainty calculated from the measured responses from a secondary source to a monitoring microphone when seats 2 and 3 are both lowered, $\Delta G_{1,2}$, and the estimate of this uncertainty, $\hat{\Delta} G_{1,2}$, calculated from the superposition of the uncertainties due to lowering seat 2 and lowering seat 3 individually.

Superposition of uncertainties is also demonstrated in Figures 9 and 10 for the case of a loudspeaker on the floor of the car, used to represent a primary source, and a monitoring microphone. The results are again encouraging, except at the frequencies at which there are dips in the frequency responses in Figure 9, where the uncertainties are less likely to be important. It should be noted that the uncertainties associated with some perturbations do not appear to superpose as accurately as these results suggest, for example when the seat 1 is moved, to which the microphones and secondary sources are attached. However, this superposition technique could still significantly cut down on the number of conditions that need to be measured in practice to evaluate robust stability and performance.

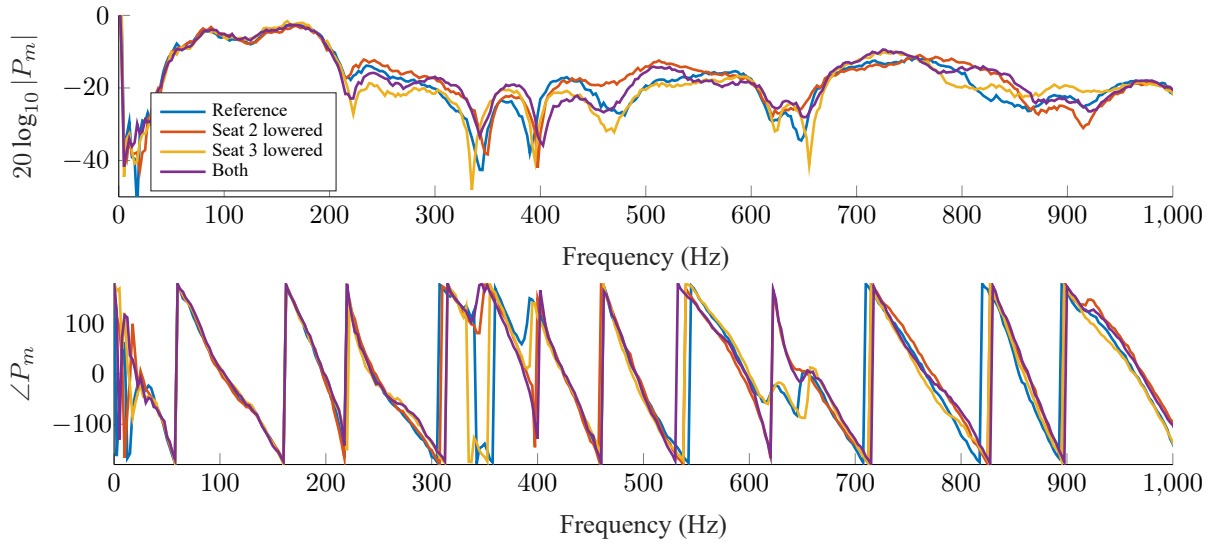

Figure 9 – Responses measured from a primary loudspeaker to a monitoring microphone under nominal conditions, Reference, when seat 2 only is lowered, when seat 3 only is lowered and when seats 2 and 3 are both lowered.

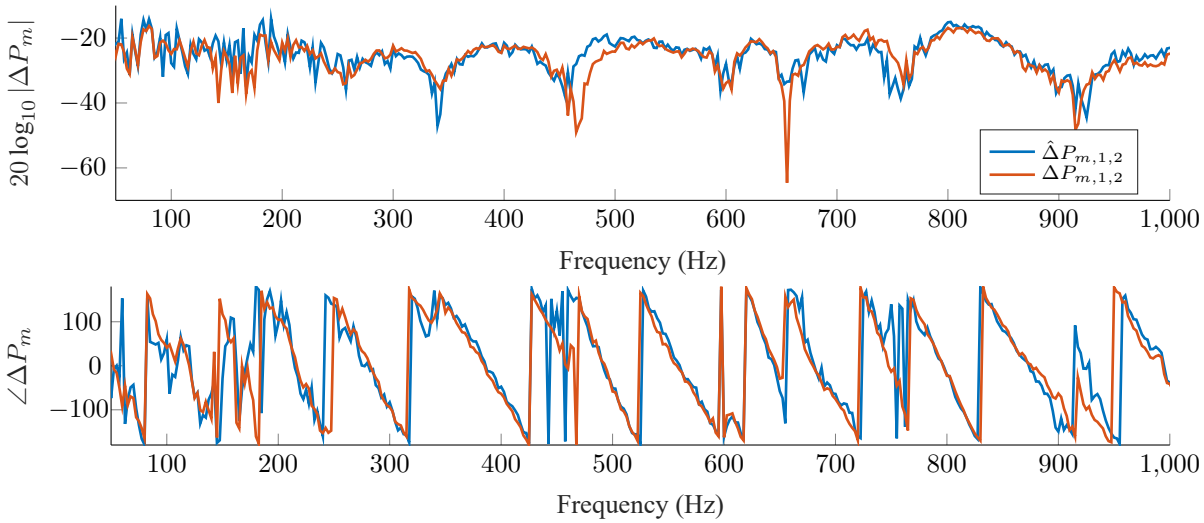

Figure 10 – The additive uncertainty measured for the response from a primary source to a monitoring microphone when seats 2 and 3 are both lowered, $\Delta P_{1,2}$, and the estimate of this uncertainty, $\Delta P_{1,2}$, calculated from the superposition of the uncertainties due to lowering seat 2 and lowering seat 3 individually.

Figure 11 shows the predicted attenuation at the error sensors, at one particular frequency, as a function of the regularisation factor, when the observation filter is calculated from the responses under nominal conditions and the performance is calculated using either the actual responses measured when both seat 2 and seat 3 were lowered, or when this is predicted using the estimated response calculated by superposition of the uncertainties due to lowering seat 2 and seat 3 individually. It can be seen that the predicted responses gives a reasonable estimate of the actual performance under these conditions, predicting that the maximum attenuation will be achieved for a regularisation parameter equal to about 10^{-2}. In this case the stability of the system is not threatened by these uncertainties but the superposition method still gives a good estimate of the two eigenvalues in Eq.(1). The variation of the attenuation with β changes from one frequency to another for the perturbed responses, but typically has its peak at a similar value of β to that seen in Figure 11 at most frequencies, indicating that robust performance, as well as robust stability, can be achieved across the frequency range with a suitable value of the regularisation parameter.

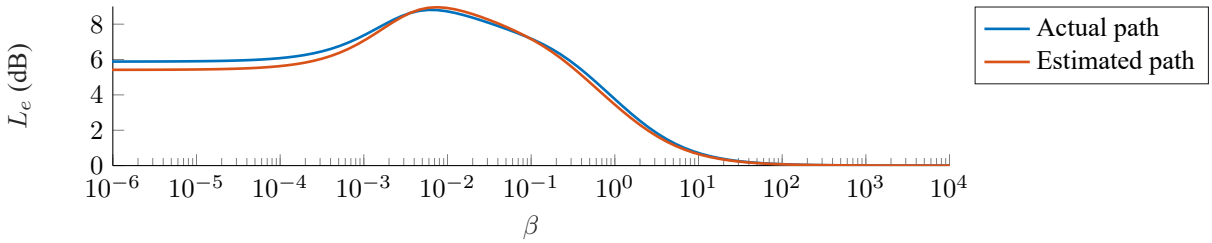

Figure 11 – The variation of the predicted attenuation at the error microphones, at a frequency of 665 Hz, with the regularisation parameter, β, used in the observation filter, designed using the responses measured under nominal conditions, but with the error calculated when both seats 2 and 3 are lowered, Actual, and evaluated when the responses with both seats lowered was calculated by superposition of the uncertainties measured when seat 2 and seat 3 were lowered individually.

5 CONCLUSIONS

A virtual sensing arrangement can be incorporated into an adaptive feedforward control system, to provide active control of the sound at a listener's ears, but without them having to wear microphones. Such an arrangement is more effective at higher frequencies than conventional local control systems, but its stability and performance then becomes more sensitive to small variations in the acoustic environment. It has been shown that for a given perturbation in the responses of the system under control, appropriate regularisation of the observation filter, used to estimate the disturbances at the error microphones from those at the monitoring microphones, can ensure both robust stability and robust performance.

The robust design process thus requires an estimate of all of the perturbed plant responses that are likely to be encountered in practice. If there are multiple sources of uncertainty, measurements of plant uncertainty under all possible combinations of conditions could be time-consuming to acquire. Another

possibility is only to measure the uncertainties due to some of the individual sources of perturbation, and then to combine these individual uncertainties to estimate the uncertainty due to different combinations of perturbation. It has been shown that under some circumstances this can be achieved by superposition of the uncertainties.

ACKNOWLEDGEMENTS

This work was supported under EPSRC Grant number EP/R006768/1: Digital twins for improved dynamic design.

REFERENCES

1. Harry F Olson and Everett G May. Electronic Sound Absorber. *The Journal of the Acoustical Society of America*, Vol 25(6), 1953.

2. Danielle Moreau, Ben Cazzolato, Anthony Zander, and Cornelis Petersen. A review of virtual sensing algorithms for active noise control. *Algorithms*, Vol 1(2):69–99, 2008.

3. Woomin Jung, Stephen J. Elliott, and Jordan Cheer. Combining the remote microphone technique with head-tracking for local active sound control. *The Journal of the Acoustical Society of America*, Vol 142 (1):298–307, 2017.

4. Stephen J. Elliott, Woomin Jung, and Jordan Cheer. Head tracking extends local active control of broadband sound to higher frequencies. *Scientific Reports*, Vol 8(1):1–7, 2018.

5. Stephen J. Elliott and Jordan Cheer. Modeling local active sound control with remote sensors in spatially random pressure fields. *The Journal of the Acoustical Society of America*, Vol 137(4):1936–1946, 2015.

6. Woomin Jung, Stephen J. Elliott, and Jordan Cheer. Local active control of road noise inside a vehicle. *Mechanical Systems and Signal Processing*, Vol 121:144–157, 2019.

7. D. Treyer, S. Gaulocher, S. Germann, and E. Curiger. Towards the implementation of the noise-cancelling office chair: Algorithms and practical aspects. In *23rd International Congress on Sound and Vibration*, 2016.

8. Stephen J. Elliott, W Jung, and Jordan Cheer. Causality and robustness in the remote sensing of acoustic pressure, with application to local active sound control. In *2019 IEEE International Conference on Acoustics, Speech and Signal Processing (ICASSP)*, pages 8484–8488, 2019.

9. Woomin Jung, Stephen J. Elliott, and Jordan Cheer. Estimation of the pressure at a listener's ears in an active headrest system using the remote microphone technique. *The Journal of the Acoustical Society of America*, Vol 143(5), 2018.